Letter

Spectroscopy of edge and bulk collective modes in fractional Chern insulators

F. Binanti,[1] N. Goldman,[2,3] and C. Repellin[4]

[1]*University Grenoble-Alpes, CNRS, LPMMC, 38000 Grenoble, France*

[2]*CENOLI, Université Libre de Bruxelles, CP 231, Campus Plaine, B-1050 Brussels, Belgium*

[3]*Laboratoire Kastler Brossel, Collège de France, CNRS, ENS-Université PSL, Sorbonne Université, 11 Place Marcelin Berthelot, 75005 Paris, France*

[4]*Univeristy Grenoble-Alpes, CNRS, LPMMC, 38000 Grenoble, France*

(Received 28 June 2023; accepted 30 January 2024; published 8 March 2024)

The exploration of atomic fractional quantum Hall (FQH) states is now within reach in optical-lattice experiments. While ground-state signatures have been observed in a system realizing the Hofstadter-Bose-Hubbard model in a box [Léonard *et al.*, Nature (London) **619**, 495 (2023)], how to access hallmark low-energy collective modes remains a central open question in this context. We introduce a spectroscopic scheme based on two interfering Laguerre-Gaussian beams, which transfer a controlled angular momentum and energy to the system. The edge and bulk responses to the probe are detected through local density measurements by tracking the transfer of atoms between the bulk and the edge of the FQH droplet. This detection scheme is shown to simultaneously reveal two specific signatures of FQH states: their chiral edge branch and their bulk magnetoroton mode. We numerically benchmark our method by considering few bosons in the $\nu = 1/2$ Laughlin ground state of the Hofstadter-Bose-Hubbard model, and demonstrate that these signatures are already detectable in realistic systems of two bosons, provided that the box potential is sufficiently large compared to the droplet. Our paper paves the way for the detection of fractional statistics in cold atoms through edge signatures.

DOI: 10.1103/PhysRevResearch.6.L012054

I. INTRODUCTION

The interplay of topology and interactions leads to fascinating phases of matter, such as the fractional quantum Hall (FQH) states, which host fractionalized anyonic excitations. The progress in engineering artificial gauge fields [1,2] and topological bands [3] has raised the hope of realizing FQH states of ultracold atoms. Specifically, realistic protocols for the preparation of FQH states were proposed [4–12] based on the quasiadiabatic evolution of a small ensemble of neutral atoms loaded into an optical lattice. In this context, extracting the universal signatures of FQH states is an important goal and great challenge; theoretical proposals in this direction have focused on the measurement of the Hall response [13–16], central charge [17], and the anyonic properties of quasiholes [18–23]. Recently, a two-particle bosonic Laughlin state was identified in an optical lattice [24], where local density measurements permitted the observation of key bulk signatures, including a nearly quantized Hall conductivity and vortex like correlations.

Edge states are a fundamental hallmark of topological matter. In FQH systems, they form one-dimensional conduction channels [25], which are responsible for a wealth of quantum coherent phenomena in mesoscopic systems [26]. Despite the success of chiral Luttinger liquid theory in capturing these phenomena, microscopic details such as boundary effects can deeply affect the low-energy picture [27–33].

Another key feature of FQH phases is their bulk collective excitations, called the magnetoroton mode (MRM), which can be viewed as a density modulation of the ground state [34,35]. Owing to the incompressibility of FQH phases, the MRM is gapped; its softening marks the transition to a Wigner crystal. While it is absent in integer quantum Hall phases, the MRM generically appears in all FQH phases.

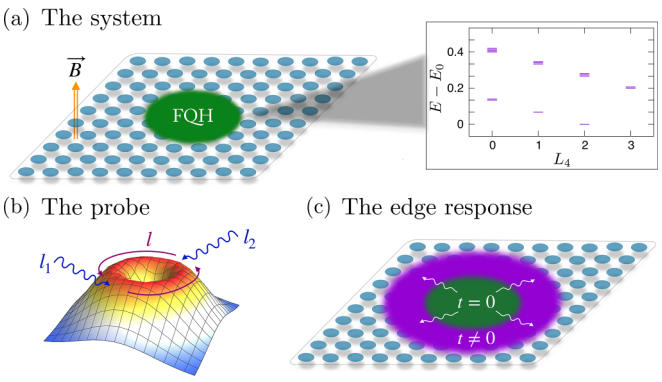

FIG. 1. (a) Fractional quantum Hall (FQH) droplet on the Hofstadter-Bose-Hubbard lattice, with a sketch of the expected edge spectrum. (b) Spatial shape of the Laguerre-Gaussian (LG) laser field acting on the atoms, realized by interfering two beams with angular momentum l_1 and l_2, and resulting in a transfer of angular momentum $l = l_1 - l_2$. (c) Response of the FQH droplet to the LG beams at resonance: edge states are populated, resulting in a detectable density increase at the droplet's edge.

Thanks to the local probes accessible in optical-lattice experiments, the realization of the FQH effect in quantum gases may provide an opportunity to reveal the rich phenomenology of FQH edge and bulk modes. Promisingly, resolving individual edge states could provide a marker of topological order, permitting the unambiguous detection of non-Abelian FQH states [36–38]. Moreover, the maximal angular momentum of the MRM could serve as an additional topological marker to distinguish FQH phases [39–43]. While edge properties have been detected in weakly interacting cold atom settings [44–48], how to extract and resolve the low-energy spectrum of FQH states remains an open question.

In this paper, we develop a spectroscopy protocol to extract the edge and bulk collective modes of FQH states in ultracold gases. Our proposal builds on Ref. [49] and is summarized in Fig. 1: two interfering Laguerre-Gaussian (LG) lasers transfer an angular momentum l and energy $\hbar\omega$ to the system prepared in the FQH ground state of a lattice Hamiltonian. The absorption resonance is subsequently measured *in situ* through local density measurements by monitoring the transfer of atoms between the bulk and edge. We numerically benchmark our protocol using the experimentally realized [24,50] Hofstadter-Bose-Hubbard (HBH) model, which supports a $\nu = 1/2$ Laughlin ground state [51–53]. By calculating the coupling matrix elements of our probe, we obtain the angular momentum resolved absorption spectrum and show that the characteristic edge and bulk collective modes are present in systems with as few as two particles. Interestingly, the LG matrix elements have an approximate selection rule corresponding to the emergent continuous rotation symmetry of low-energy states. This property allows us to extract the edge and bulk modes even when they are energetically mixed. Upon approaching the experimental configuration of Ref. [24], the walls of the confining box nearly coincide with the edge of the FQH droplet, leading to a gapped edge mode lying higher in energy than the first bulk excitation. The explicit time-dependent simulation of our protocol shows that the time necessary to detect a measurable transfer of density from bulk to edge is compatible with current experimental constraints. Our protocol could apply to other models of FQH states of ultracold atoms, including rotating atomic traps [48].

II. MODEL

We consider the HBH model, describing bosons hopping on the Harper-Hofstadter lattice [54] and interacting through an on-site Hubbard interaction of strength $U > 0$,

$$\begin{aligned}\hat{H} = &-J\sum_{m,n}(\hat{b}^\dagger_{m+1,n}\hat{b}_{m,n}e^{i2\pi\alpha n} + \hat{b}^\dagger_{m,n+1}\hat{b}_{m,n} + \text{H.c.}) \\ &+ \frac{U}{2}\sum_{m,n}\hat{b}^\dagger_{m,n}\hat{b}_{m,n}(\hat{b}^\dagger_{m,n}\hat{b}_{m,n} - 1) \\ &+ \sum_{m,n}V(m,n)\hat{b}^\dagger_{m,n}\hat{b}_{m,n}, \end{aligned} \tag{1}$$

where the operator $\hat{b}_{m,n}$ ($\hat{b}^\dagger_{m,n}$) destroys (creates) a boson at site (m, n), J is the tunneling energy, α is the magnetic flux density, and $V(m, n) = V_0((m - m_0)^2 + (n - n_0)^2)$ is a confining potential (m_0, n_0 are the coordinates of the lattice center). Throughout the paper, we work in the strong interaction regime $U \gg J = 1$ and use hardcore bosons in the numerics unless otherwise stated. For $\alpha < 1/3$, this model hosts a fractional Chern insulator ground state [51–53], which is a lattice analog of the $\nu = 1/2$ bosonic Laughlin state. A cold-atom implementation of this model was realized using two bosons in a box potential [24,50], revealing signatures of the Laughlin FQH state [24].

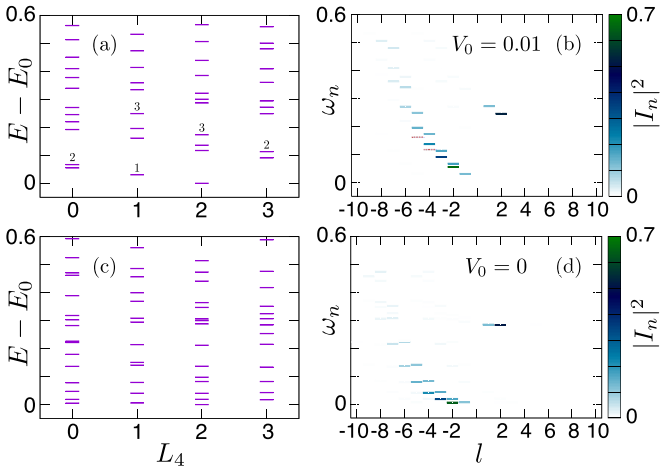

FIG. 2. Low-energy spectrum (a), (c) and corresponding coupling matrix elements I_n (b), (d) for a system of two hardcore bosons in the HBH model at flux density $\alpha = 1/8$ in a 10 x 10 box, with (a), (b) or without (c), (d) a harmonic potential of strength $V_0 = 0.01$. ω_n is the energy difference between excited and ground states. Unlike the energy spectrum, the matrix elements always distinguish edge and bulk modes, regardless of the presence of a harmonic potential. The numbers in (a) indicate the number of states in each cluster, which matches the CFT counting with finite particle number correction. While matrix elements to all excited states are shown in (b), (d), the small $|I_n|$ sometimes precludes their visualization. We have added a red dashed line wherever necessary to identify the edge counting.

We start by reviewing the properties of the FQH edge spectrum. In the low-energy limit, the edge modes of FQH states are described by a conformal field theory (CFT), whose nature depends on the topological order in the bulk [25,36,37,55]; for the Laughlin state considered here, it coincides with the chiral Luttinger liquid. This powerful bulk-edge correspondence can be harnessed to identify FQH states from their low-energy spectrum, which reveals the universal counting of the CFT (the number of low-energy edge states for each momentum value). Extracting the edge spectrum is a nontrivial task, even numerically. Previous numerical studies have shown that a gapless chiral edge mode, whose counting matches the CFT expectation [32,33], could be extracted from the energy spectrum in the presence of a smooth confining potential. Interestingly, this property is already present in two-boson systems, with corrections to the CFT counting due to finite particle number [33,56]. This is illustrated in Fig. 2(a), through the low-energy spectrum of two bosons in the HBH model in a weak harmonic trap, using the eigenvalues of the modified C_4 rotation operator [57] to highlight the chirality of the edge spectrum. The situation is different in a box potential, where the absence of low-energy structure prevents the extraction of the edge spectrum; see Fig. 2(c) and Refs. [13,32]. We

now show how chiral edge and bulk properties can nonetheless be extracted in these relevant configurations, using a proper spectroscopic probe.

A. Optical spectroscopy

We propose to probe the FQH edge and bulk modes by using two interfering LG lasers designed to induce a transition from the prepared FQH ground state to low-energy excitations. This transition involves a transfer of angular momentum l and energy $\hbar\omega$, which are conveniently controlled by the pair of LG beams [58] (Fig. 1). This differs from the detection scheme of Refs. [29,59], where the dispersion relation is extracted through a Fourier transform of the particle density following a quench. Such a LG-driving scheme was initially proposed in Ref. [49] to probe the edge spectrum of integer QH states. Beyond the strongly interacting nature of the FQH state treated in this paper, the small system sizes envisaged to realize FQH states in experiments results in a highly discretized spectrum. Our proposed scheme takes these key properties into account, and we discuss their consequences on the resulting absorption spectrum.

The LG modes are solutions of the cylindrical-symmetric wave equation and take the following form:

$$\mathrm{LG}(r,\theta) \propto \left(\frac{r}{r_0}\right)^{|l|} e^{-\frac{r^2}{2r_0^2}} e^{i\theta l} \equiv f_l(r) e^{i\theta l}, \tag{2}$$

where the integer l represents the quantum of orbital angular momentum carried by each photon. As shown in Fig. 1(b), such an optical mode has a spatial vortex structure, with a ring of maximum amplitude that can be adjusted to optimize the edge response. The interference of two such LG beams, with frequencies ω_1, ω_2 and angular momenta l_1, l_2 produces a time-periodic potential acting on the atoms,

$$\hat{O}_l(t) = 2\epsilon \sum_j f_l(r_j) \cos\left(\omega t + \theta_j l\right) \hat{b}_j^\dagger \hat{b}_j, \tag{3}$$

where j sums over the lattice sites, θ_j is the polar angle at j, $\omega = \omega_2 - \omega_1$ and $l = l_2 - l_1$.

To predict allowed transitions, we calculate the coupling of the FQH ground state ψ_0 to excitations ψ_n through the LG drive, i.e., the coupling matrix elements:

$$I_n = \sum_j \langle \psi_n | f_l(r_j) e^{i\theta_j l} \hat{b}_j^\dagger \hat{b}_j | \psi_0 \rangle. \tag{4}$$

We calculate the low-energy eigenstates of $\hat{H}$ for a system of $N = 2$ hard-core bosons on a 10 x 10 lattice with magnetic flux $\alpha = 1/8$ using exact diagonalization (ED). The corresponding low-energy spectrum and matrix elements I_n are represented in Fig. 2 for a harmonic and a box potential, respectively. In both cases, the matrix elements exhibit a chiral branch at $l < 0$, and two isolated gapped states at $l = 1$ and $l = 2$. We interpret the gapless $l < 0$ branch as the chiral edge mode; as expected, the sign of orbital angular momentum injected by the probe matches the chirality of the edge boson. Conversely, the $l > 0$ signal is interpreted as low-energy bulk excitations, which correspond to the MRM [35]. While the maximum value of $|l|$ in the edge mode is dictated by the lattice size (here, the 10 x 10 box), giving rise to a large number of low-energy edge states, the number of MRM states above the Laughlin state is equal to the number of particles [43,60,61]. The analysis of density profiles (below in the main text, and in Ref. [61]) corroborates this interpretation of negative and positive l states as edge and bulk states, respectively.

Interestingly, the LG probe identifies the chiral branch and MRM even when no structure can be extracted from the low-energy ED spectrum [Figs. 2(c) and 2(d)]. This behavior originates from the approximate rotation symmetry of the low-energy eigenstates. While the discrete C_4 rotation symmetry of our lattice model only guarantees the conservation of the angular momentum l modulo 4, l is approximately conserved. At small α, reduced lattice effects lead to a better conservation of l [61]. Yet, even for the experimentally relevant regime $\alpha \approx 1/4$, coupling matrix elements that satisfy the conservation of l mod 4 but not the conservation of l are 40 times smaller than those that do. Overall, Figs. 2(b) and 2(d) show that the addition of a weak harmonic potential increases the velocity of the chiral edge mode, such that its winding becomes visible in the folded energy spectrum [Fig. 2(a)].

We have chosen the value $r_0 = 2$ for the Gaussian extension of the probe such that $f_l(r)$ remains nonzero both in the bulk and a few magnetic lengths outside the edge of the FQH droplet, at least for $|l| \leqslant 5$. This is a necessary condition for the corresponding matrix elements to be nonzero, due to the density profiles of the ground state and low-energy excited states, whose spatial extension increases with increasing energy [61]. Naturally, the optimal value of r_0 depends on the size of the droplet; in larger droplets, it is especially useful to optimize r_0 to specific values of l [61].

B. Connection to the Harvard experiment

We now apply our spectroscopy protocol to the experimental setup of Ref. [24]. There, $N = 2$ interacting ($U = 8.1J$) bosons are confined to a 4 x 4 box with hard walls on the HBH lattice, and a FQH ground state was identified within a flux window $0.24 < \alpha < 0.3$. Focusing on $\alpha = 0.25$, we show our probe's matrix elements in Fig. 3(a). The absorption spectrum is consistent with a FQH state whose edge mode is gapped due to the small size of the box. Releasing the walls of the 4 x 4 box into a 10 x 10 box confirms this interpretation: the $l < 0$ edge branch goes down and becomes gapless, while the $l = 2$ bulk gap increases; see Fig. 3, with the trap shape drawn as an inset. Further numerical investigation [61] shows that in a large box, irrespective of the trap shape, the FQH droplet recovers a gapless edge mode, and its bulk gap increases until it reaches its thermodynamic value. Conversely, when the size of the box is reduced, the bulk gap decreases and eventually closes, marking a phase transition. Overall, our calculations show that increasing the size of the quantum-simulation box could permit the observation of a chiral gapless edge mode in ongoing experiments, even in two-atom droplets.

C. Extracting the edge and bulk modes from *in situ* density measurements

We now show how to obtain the absorption spectrum studied in the previous paragraphs using observables accessible to cold-atom experiments.

Due to its well-defined angular momentum l, our LG probe only couples the ground state to a handful of excited states at

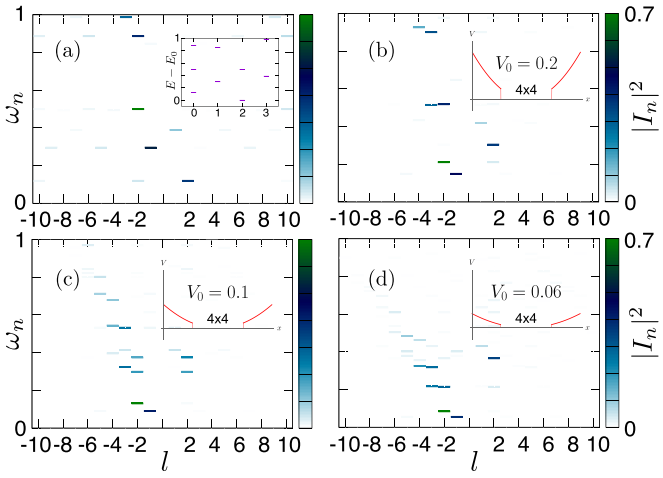

FIG. 3. Absorption spectra for $N=2$ interacting bosons ($U = 8.1J$) on a 10 x 10 HBH lattice with flux $\alpha = 0.25$, and different trap configurations, keeping $V_0=0$ in the central 4 x 4 portion of the lattice. (a) Harvard experiment configuration [24], with infinite walls around the 4 x 4 box. The inset shows the corresponding energy spectrum. (b)–(d) Harmonic potential of respective strength $V_0=0.2, 0.1, 0.06$. Upon lowering the potential in the outer box, the bulk gap ($l=2$ signal) increases, while the edge branch ($l<0$) becomes gapless. The weak signal at $l=2$, at the same energy as the $l=-2$ edge signal is due to the imperfect conservation of l.

most, as observed in our analysis of transition matrix elements I_n. As a result, the LG drive induces an effective two-level coupling for each value of l. Using unitary time-evolution of the FQH ground state subjected to the LG drive, we numerically observe Rabi oscillations, whose amplitude is maximal at the resonance frequency $\omega = \omega_{\rm res}$ [Fig. 4(a)].

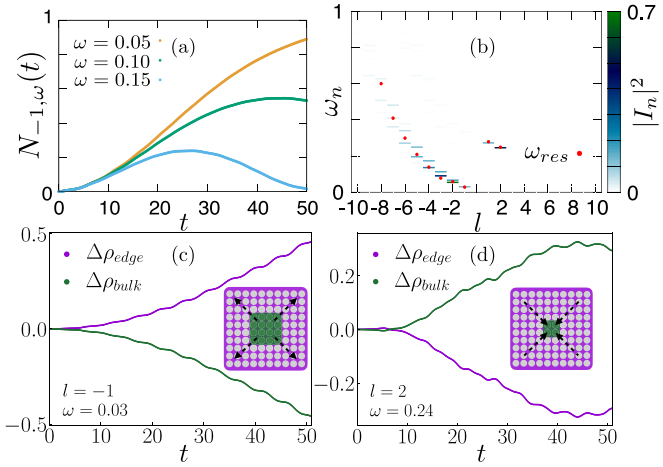

FIG. 4. Time evolution of two hardcore bosons on a 10 x 10 HBH lattice with flux $\alpha = 1/8$ and a harmonic trap of strength $V_0 = 0.01$, upon a LG drive of amplitude $\epsilon = 0.05$. (a) Excitation fraction $N_{l,\omega}(t) = 1 - |\langle\psi(t)|\psi_0\rangle|^2$ for an injected angular momentum $l=-1$. (b) Chiral branch and magnetoroton mode extracted from the density-transfer protocol (dots). Colored bars indicate the coupling matrix elements. (c), (d) Density variation at the edge and bulk, for $l=-1$ and $l=2$, representative of the typical resonant coupling to edge and bulk states.

We propose to detect the resonant excitations through local density measurements, which are experimentally accessible using a quantum gas microscope [24,50]. Following the excitation of edge states, we expect the density profile to increasingly populate the external rings outside the bulk. Conversely, we expect transitions to the MRM to result in a density increase in the bulk due to its nature as a compressibility modulation of the ground state [61] We define the instantaneous edge density as

$$\Delta\rho_{\rm edge}(t) = \sum_{j\in{\rm edge}} \rho_j(t) - \rho_j(0), \tag{5}$$

where ρ_j is the density on site j, and we have defined the complementary bulk and edge regions [green and purple regions in the inset of Figs. 4(c) and 4(d)] from the ground-state density profile [61]. The time-dependent behavior of $\Delta\rho_{\rm edge}(t)$, as obtained using numerical time evolution in Figs. 4(c) and 4(d), confirms the migration of the particle density from bulk to edge (respectively edge to bulk) for a negative (respectively positive) injected angular momentum. Figures 4(c) and 4(d) show the evolution of $\Delta\rho_{\rm edge}$ and $\Delta\rho_{\rm bulk}$ at the resonance frequency and angular momentum for, respectively, the edge state at $l=1$ and MRM state at $l=2$. Iterating this procedure for different values of the injected angular momentum l, we retrieve the chiral edge spectrum and MRM in Fig. 4(b). The observation time at which we extract the resonance frequencies for $l<0$ is $t^*=50\hbar/J$. We point out that a realistic observation time $t^*\sim 10-100\hbar/J$ leads to a clear signal $\Delta\rho_{\rm edge}(t^*)\sim 0.1-1$, which can be detected using a quantum gas microscope [24]. We also verified the ability of our protocol to detect edge signals in the experimental configuration of Ref. [24]; see Ref. [61]. Lastly, performing a full transfer to a target edge state would allow to image its hallmark vortex structure *in situ* [61].

III. DISCUSSION

Our paper indicates that the chiral edge branch and MRM of atomic FQH droplets can be probed by measuring the local density following a LG drive. Our method is well-suited to probe the few-atom droplets addressed by ongoing experiments. Increasing the lattice size beyond the small boxes realized so far in experiments [24] would permit the extraction of a gapless edge mode even in two-particle systems. We have verified the validity of our results beyond this limit, for three or four particles, where we can still address very dilute systems [61]. Beyond experimental purposes, the calculation of LG matrix elements is a convenient tool to analyze bulk and edge properties of FQH states, especially in lattice systems without continuous rotation symmetry. It distinguishes bulk and edge states, allowing, e.g., the tracking of the bulk gap and of the velocity of the edge branch upon changing the confining conditions.

Finally, our method is promising in view of identifying the fractional statistics of anyonic excitations (see also Ref. [18]). Indeed, the number of edge states detected by our LG probe for each value of the angular momentum l matches the CFT counting for a free chiral boson (with corrections due to the small particle number [33]), which describes the edge of a Laughlin droplet. We have verified that a tighter confinement

of the FQH droplet leads to larger energy splittings, permitting the resolution of resonances occurring at the same l without requiring longer observation times [61]. Overall, our scheme allows us to extract the edge counting at least up to $l=-3$, which is enough to distinguish most FQH states [62] The MRM constitutes an additional topological signature, absent from integer quantum Hall phases, and whose maximum angular momentum distinguishes between different FQH phases [63].

ACKNOWLEDGMENTS

We thank B. Bakkali-Hassani, J. Dalibard, A. Eckardt, M. Greiner, F. Grusdt, A. G. Grushin, M. Holzmann, J. Kwan, J. Léonard, Y. Li, F. Palm, P. Segura, and B. Wang for insightful discussions. C.R. acknowledges support from ANR through Grant No. ANR-22-CE30-0022-01. Work in Brussels is supported by the FRS-FNRS (Belgium), the ERC Starting Grants TopoCold and LATIS, and the EOS project CHEQS.

[1] J. Dalibard, F. Gerbier, G. Juzeliūnas, and P. Öhberg, Colloquium: Artificial gauge potentials for neutral atoms, Rev. Mod. Phys. **83**, 1523 (2011).

[2] N. Goldman, G. Juzeliūnas, P. Öhberg, and I. B. Spielman, Light-induced gauge fields for ultracold atoms, Rep. Prog. Phys. **77**, 126401 (2014).

[3] N. R. Cooper, J. Dalibard, and I. B. Spielman, Topological bands for ultracold atoms, Rev. Mod. Phys. **91**, 015005 (2019).

[4] M. Popp, B. Paredes, and J. I. Cirac, Adiabatic path to fractional quantum Hall states of a few bosonic atoms, Phys. Rev. A **70**, 053612 (2004).

[5] N. R. Cooper and J. Dalibard, Reaching fractional quantum Hall states with optical flux lattices, Phys. Rev. Lett. **110**, 185301 (2013).

[6] N. Y. Yao, A. V. Gorshkov, C. R. Laumann, A. M. Läuchli, J. Ye, and M. D. Lukin, Realizing fractional Chern insulators in dipolar spin systems, Phys. Rev. Lett. **110**, 185302 (2013).

[7] F. Grusdt, F. Letscher, M. Hafezi, and M. Fleischhauer, Topological growing of Laughlin states in synthetic gauge fields, Phys. Rev. Lett. **113**, 155301 (2014).

[8] Y.-C. He, F. Grusdt, A. Kaufman, M. Greiner, and A. Vishwanath, Realizing and adiabatically preparing bosonic integer and fractional quantum Hall states in optical lattices, Phys. Rev. B **96**, 201103(R) (2017).

[9] C. Repellin, T. Yefsah, and A. Sterdyniak, Creating a bosonic fractional quantum Hall state by pairing fermions, Phys. Rev. B **96**, 161111(R) (2017).

[10] J. Motruk and F. Pollmann, Phase transitions and adiabatic preparation of a fractionalChern insulator in a boson cold-atom model, Phys. Rev. B **96**, 165107 (2017).

[11] A. Hudomal, N. Regnault, and I. Vasić, Bosonic fractional quantum Hall states in driven optical lattices, Phys. Rev. A **100**, 053624 (2019).

[12] B. Michen, C. Repellin, and J. C. Budich, Adiabatic preparation of fractional Chern insulators from an effective thin-torus limit, Phys. Rev. Res. **5**, 023100 (2023).

[13] C. Repellin and N. Goldman, Detecting fractional Chern insulators through circular dichroism, Phys. Rev. Lett. **122**, 166801 (2019).

[14] C. Repellin, J. Léonard, and N. Goldman, Fractional Chern insulators of few bosons in a box: Hall plateaus from center-of-mass drifts and density profiles, Phys. Rev. A **102**, 063316 (2020).

[15] J. Motruk and I. Na, Detecting fractional Chern insulators in optical lattices through quantized displacement, Phys. Rev. Lett. **125**, 236401 (2020).

[16] Z.-P. Cian, H. Dehghani, A. Elben, B. Vermersch, G. Zhu, M. Barkeshli, P. Zoller, and M. Hafezi, Many-body Chern number from statistical correlations of randomized measurements, Phys. Rev. Lett. **126**, 050501 (2021).

[17] F. A. Palm, S. Mardazad, A. Bohrdt, U. Schollwöck, and F. Grusdt, Snapshot-based detection of $\nu=\frac{1}{2}$ Laughlin states: Coupled chains and central charge, Phys. Rev. B **106**, L081108 (2022).

[18] N. R. Cooper and S. H. Simon, Signatures of fractional exclusion statistics in the spectroscopy of quantum Hall droplets, Phys. Rev. Lett. **114**, 106802 (2015).

[19] M. Račiūnas, F. N. Ünal, E. Anisimovas, and A. Eckardt, Creating, probing, and manipulating fractionally charged excitations of fractional Chern insulators in optical lattices, Phys. Rev. A **98**, 063621 (2018).

[20] R. O. Umucalılar, E. Macaluso, T. Comparin, and I. Carusotto, Time-of-flight measurements as a possible method to observe anyonic statistics, Phys. Rev. Lett. **120**, 230403 (2018).

[21] E. Macaluso, T. Comparin, R. O. Umucalılar, M. Gerster, S. Montangero, M. Rizzi, and I. Carusotto, Charge and statistics of lattice quasiholes from density measurements: A tree tensor network study, Phys. Rev. Res. **2**, 013145 (2020).

[22] B. Wang, X.-Y. Dong, and A. Eckardt, Measurable signatures of bosonic fractional Chern insulator states and their fractional excitations in a quantum-gas microscope, SciPost Phys. **12**, 095 (2022).

[23] X. Li, B. Jaworowski, M. Haque, and A. E. B. Nielsen, Dynamics of quasiholes and quasiparticles at the edges of small lattices, Phys. Rev. A **109**, 023312 (2024).

[24] J. Léonard, S. Kim, J. Kwan, P. Segura, F. Grusdt, C. Repellin, N. Goldman, and M. Greiner, Realization of a fractional quantum Hall state with ultracold atoms, Nature (London) **619**, 495 (2023).

[25] X. G. Wen, Chiral Luttinger liquid and the edge excitations in the fractional quantum Hall states, Phys. Rev. B **41**, 12838 (1990).

[26] C. Bäuerle, D. C. Glattli, T. Meunier, F. Portier, P. Roche, P. Roulleau, S. Takada, and X. Waintal, Coherent control of single electrons: A review of current progress, Rep. Prog. Phys. **81**, 056503 (2018).

[27] E. Macaluso and I. Carusotto, Hard-wall confinement of a fractional quantum Hall liquid, Phys. Rev. A **96**, 043607 (2017).

[28] R. Fern and S. H. Simon, Quantum Hall edges with hard confinement: Exact solution beyond Luttinger liquid, Phys. Rev. B **95**, 201108(R) (2017).

[29] X.-Y. Dong, A. G. Grushin, J. Motruk, and F. Pollmann, Charge excitation dynamics in bosonic fractional Chern insulators, Phys. Rev. Lett. **121**, 086401 (2018).
[30] A. Nardin and I. Carusotto, Linear and nonlinear edge dynamics of trapped fractional quantum Hall droplets, Phys. Rev. A **107**, 033320 (2023).
[31] B. Oblak, B. Lapierre, P. Moosavi, J.-M. Stéphan, and B. Estienne, Anisotropic quantum Hall droplets, arXiv:2301.01726.
[32] J. A. Kjäll and J. E. Moore, Edge excitations of bosonic fractional quantum Hall phases in optical lattices, Phys. Rev. B **85**, 235137 (2012).
[33] W.-W. Luo, W.-C. Chen, Y.-F. Wang, and C.-D. Gong, Edge excitations in fractional Chern insulators, Phys. Rev. B **88**, 161109(R) (2013).
[34] S. M. Girvin, A. H. MacDonald, and P. M. Platzman, Collective-excitation gap in the fractional quantum Hall effect, Phys. Rev. Lett. **54**, 581 (1985).
[35] S. M. Girvin, A. H. MacDonald, and P. M. Platzman, Magneto-roton theory of collective excitations in the fractional quantum Hall effect, Phys. Rev. B **33**, 2481 (1986).
[36] G. Moore and N. Read, Nonabelions in the fractional quantumHall effect, Nucl. Phys. B **360**, 362 (1991).
[37] X.-G. Wen, Topological order and edge structure of $\nu = 1/2$ quantum Hall state, Phys. Rev. Lett. **70**, 355 (1993).
[38] M. Milovanović and N. Read, Edge excitations of paired fractional quantum Hall states, Phys. Rev. B **53**, 13559 (1996).
[39] R. K. Kamilla, X. G. Wu, and J. K. Jain, Excitons of composite fermions, Phys. Rev. B **54**, 4873 (1996).
[40] I. D. Rodriguez, A. Sterdyniak, M. Hermanns, J. K. Slingerland, and N. Regnault, Quasiparticles and excitons for the Pfaffian quantum Hall state, Phys. Rev. B **85**, 035128 (2012).
[41] B. Yang, Z.-X. Hu, Z. Papić, and F. D. M. Haldane, Model wave functions for the collective modes and the magnetoroton theory of the fractional quantum Hall effect, Phys. Rev. Lett. **108**, 256807 (2012).
[42] B. Yang, Analytic wave functions for neutral bulk excitations in fractional quantum Hall fluids, Phys. Rev. B **87**, 245132 (2013).
[43] T. Jolicoeur, Shape of the magnetoroton at $\nu = 1/3$ and $\nu = 7/3$ in real samples, Phys. Rev. B **95**, 075201 (2017).
[44] M. Mancini, G. Pagano, G. Cappellini, L. Livi, M. Rider, J. Catani, C. Sias, P. Zoller, M. Inguscio, M. Dalmonte, and L. Fallani, Observation of chiral edge states with neutral fermions in synthetic Hall ribbons, Science **349**, 1510 (2015).
[45] B. K. Stuhl, H.-I. Lu, L. M. Aycock, D. Genkina, and I. B. Spielman, Visualizing edge states with an atomic Bose gas in the quantum Hall regime, Science **349**, 1514 (2015).
[46] T. Chalopin, T. Satoor, A. Evrard, V. Makhalov, J. Dalibard, R. Lopes, and S. Nascimbene, Probing chiral edge dynamics and bulk topology of a synthetic Hall system, Nat. Phys. **16**, 1017 (2020).
[47] C. Braun, R. Saint-Jalm, A. Hesse, J. Arceri, I. Bloch, and M. Aidelsburger, Real-space detection and manipulation of topological edge modes with ultracold atoms, arXiv:2304.01980.
[48] R. Yao, S. Chi, B. Mukherjee, A. Shaffer, M. Zwierlein, and R. J. Fletcher, Observation of chiral edge transport in a rapidly-rotating quantum gas, arXiv:2304.10468.
[49] N. Goldman, J. Beugnon, and F. Gerbier, Detecting chiral edge states in the Hofstadter optical lattice, Phys. Rev. Lett. **108**, 255303 (2012).
[50] M. E. Tai, A. Lukin, M. Rispoli, R. Schittko, T. Menke, Dan Borgnia, P. M. Preiss, F. Grusdt, A. M. Kaufman, and M. Greiner, Microscopy of the interacting Harper-Hofstadter model in the two-body limit, Nature (London) **546**, 519 (2017).
[51] A. S. Sorensen, E. Demler, and M. D. Lukin, Fractional quantum Hall states of atoms in optical lattices, Phys. Rev. Lett. **94**, 086803 (2005).
[52] M. Hafezi, A. S. Sørensen, E. Demler, and M. D. Lukin, Fractional quantum Hall effect in optical lattices, Phys. Rev. A **76**, 023613 (2007).
[53] M. Gerster, M. Rizzi, P. Silvi, M. Dalmonte, and S. Montangero, Fractional quantum Hall effect in the interacting Hofstadter model via tensor networks, Phys. Rev. B **96**, 195123 (2017).
[54] D. R. Hofstadter, Energy levels and wave functions of Bloch electrons in rational and irrational magnetic fields, Phys. Rev. B **14**, 2239 (1976).
[55] A. Nardin, R. Lopes, M. Rizzi, L. Mazza, and S. Nascimbene, Bisognano-Wichmann Hamiltonian for the entanglement spectroscopy of fractional quantum Hall states, arXiv:2312.07604.
[56] For two particles, the counting for a free chiral boson (1, 1, 2, 3, 5, 7 . . .) is truncated down to (1, 1, 2, 2, 3, 3 . . .).
[57] T. Ozawa, H. M. Price, and I. Carusotto, Momentum-space Harper-Hofstadter model, Phys. Rev. A **92**, 023609 (2015).
[58] H. He, M. E. J. Friese, N. R. Heckenberg, and H. Rubinsztein-Dunlop, Direct observation of transfer of angular momentum to absorptive particles from a laser beam with a phase singularity, Phys. Rev. Lett. **75**, 826 (1995).
[59] B.-Y. Sun, N. Goldman, M. Aidelsburger, and M. Bukov, Engineering and probing non-Abelian chiral spin liquids using periodically driven ultracold atoms, PRX Quantum **4**, 020329 (2023).
[60] C. Repellin, T. Neupert, Z. Papić, and N. Regnault, Single-mode approximation for fractional Chern insulators and the fractional quantum Hall effect on the torus, Phys. Rev. B **90**, 045114 (2014).
[61] See Supplemental Material at http://link.aps.org/supplemental/10.1103/PhysRevResearch.6.L012054 for additional numerical results, including the influence of lattice effects, time-dependent simulations in the configuration of the Harvard experiment, local density patterns, and absorption spectra for three and four bosons.
[62] The counting is, respectively, (1, 1, 2, 3) and (1, 1, 3, 5) for the Laughlin and Moore-Read states.
[63] $L_{\max} = N$ and $L_{\max} = N/2$ are, respectively, expected for Laughlin and Moore-Read.